Realizing and Probing Artificial Gauge Fields with Ultracold Atoms

Monika Aidelsburger, Marcos Atala, Michael Lohse, Christian Schweizer, Julio Barreiro

Christian Gross, Stefan Kuhr, Manuel Endres, Marc Cheneau,
Takeshi Fukuhara, Peter Schauss, Sebastian Hild, Johannes Zeiher

Ulrich Schneider, Simon Braun, Philipp Ronzheimer,
Michael Schreiber, Tim Rom, Sean Hodgman

Ulrich Schneider, Monika Schleier-Smith, Lucia Duca, Tracy Li, Martin Reitter,
Josselin Bernadoff, Henrik Lüschen, Jakob Näger

Ahmed Omran, Martin Boll, Timon Hilker, Michael Lohse,
Thomas Reimann, Alexander Keesling, Christian Gross

Simon Fölling, Francesco Scazza, Christian Hofrichter,
Pieter de Groot, Moritz Höfer

Christoph Gohle, Tobias Schneider, Nikolaus Buchheim, Zhenkai Lu

Humboldt Research Awardees:
N. Cooper, C. Salomon, W. Ketterle, E. Demler

Max-Planck-Institut für Quantenoptik
Ludwig-Maximilians Universität

funding by
€ MPG, European Union, DFG
$ DARPA (OLE)

erc synergy

www.quantum-munich.de

Outline

Realizing Artificial Gauge Fields

1. Realizing the Hoftstadter & Quantum Spin Hall Hamiltonian
2. Measuring Chern Numbers through Bulk Topological Currents
3. Probing Meissner Currents in Flux Ladders

Probing Topological Features of Bloch Bands

4. Probing Zak Phases in Topological Bands
5. Probing Band Topology using Atom Interferometry
'Aharonov Bohm', 'Wilson Loops' & 'Stückelberg'

Introduction **Optical Lattice Potential – Perfect Artificial Crystals**

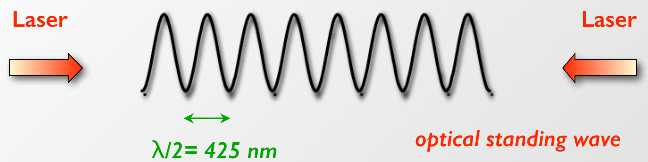

Fourier synthesize arbitrary lattices:

- Square
- Hexagonal/Triangular/Brick Wall
- Kagomé
- Superlattices
- *Spin dependent lattices*
- ...

Special case:
flux lattices...

Full **dynamical** control over **lattice depth, geometry, dimensionality!**

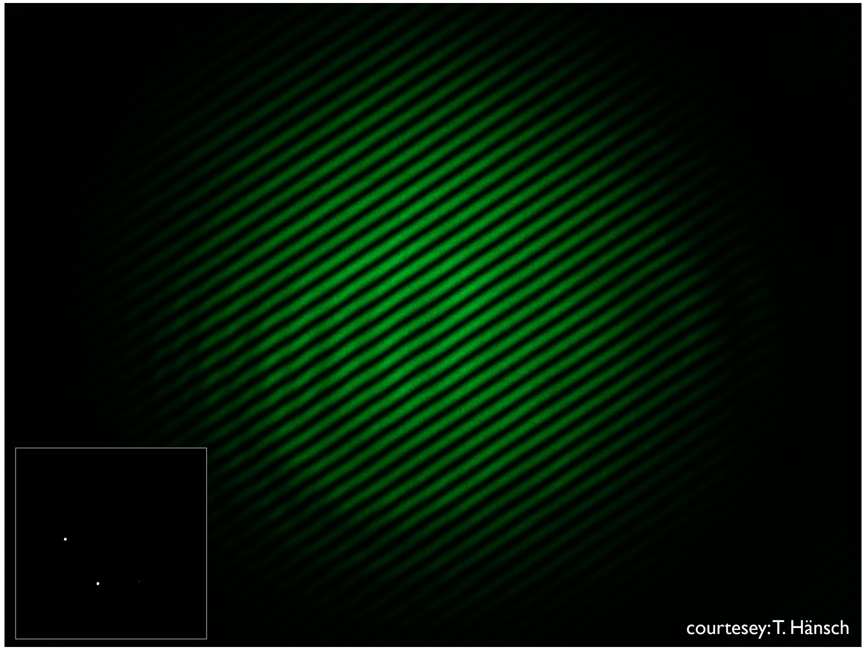

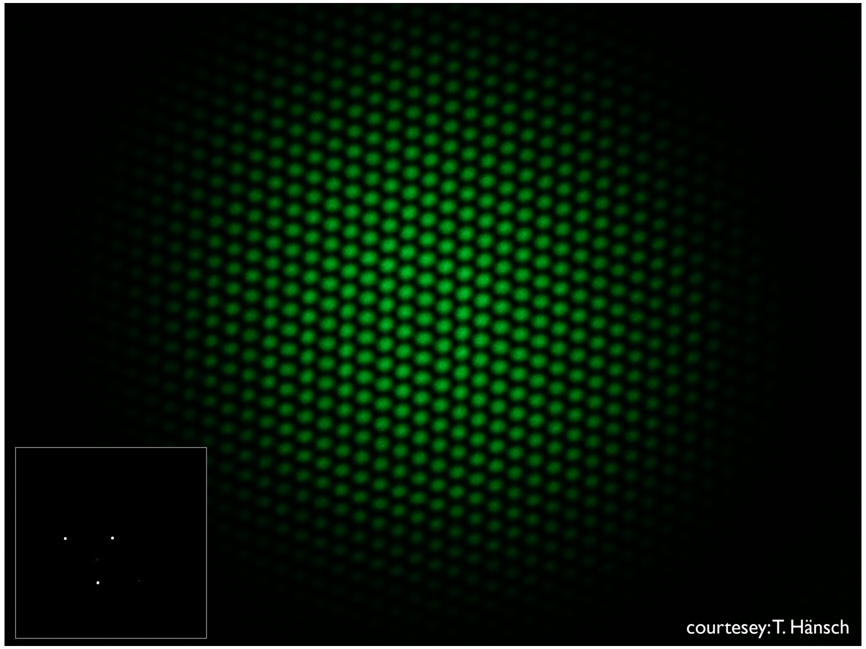

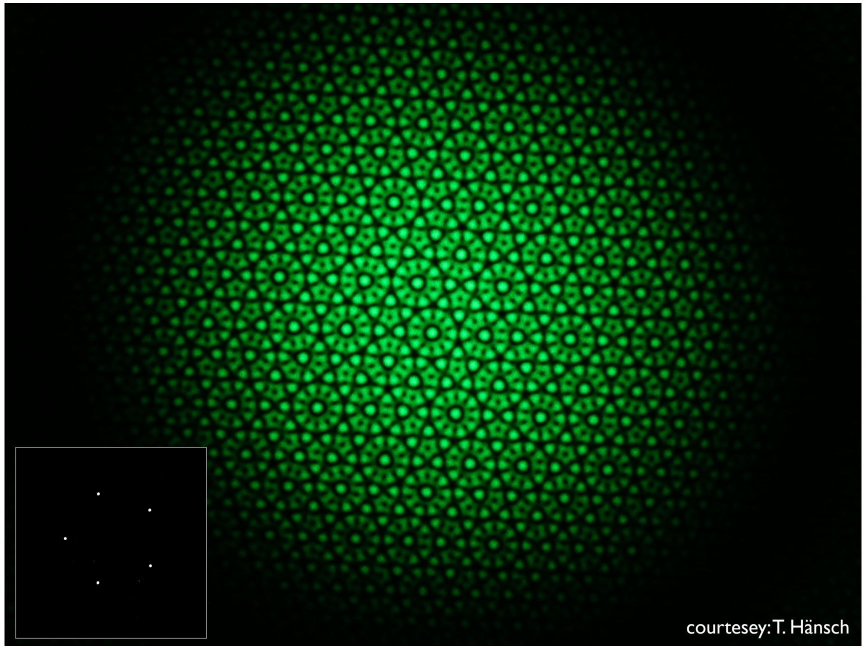

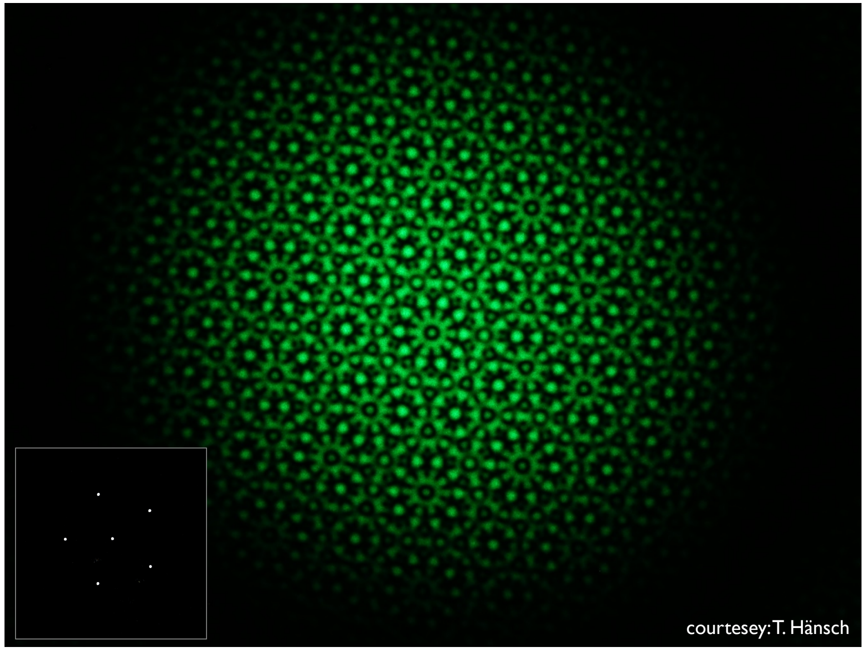

Tuning Interactions

^{39}K-^{39}K Feshbach resonance

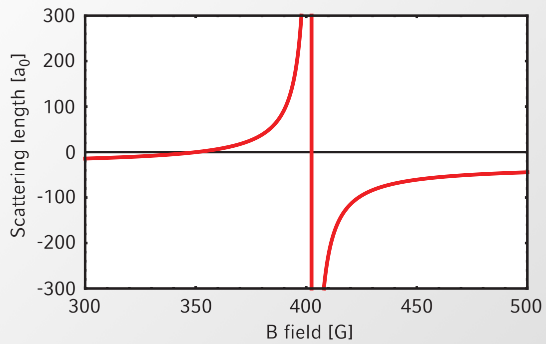

Short ranged s-wave interactions!

Watch out for inelastic collisions (three body losses...)!

Feshbach resonance allow us to control interactions!

Chin, C., Grimm, R., Julienne, P. & Tiesinga, E. *Rev. Mod. Phys.* **82**, 1225–1286 (2010).

ERC Synergy — From Artificial Quantum Matter to Real Materials

Quantum Regime

/ ≳

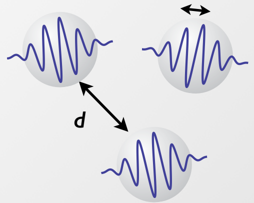

Universality of Quantum Mechanics!

Ultracold Quantum Matter

- **Densities:** $10^{14}/cm^3$ (100000 times thinner than air)
- **Temperatures:** few nK (100 million times lower than outer space)

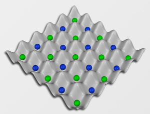

Real Materials

- **Densities:** 10^{24}-$10^{25}/cm^3$
- **Temperatures:** mK – several hundred K

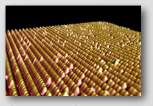
(Neuchatel)

Same / !

Single Atoms — Measuring a Quantum System

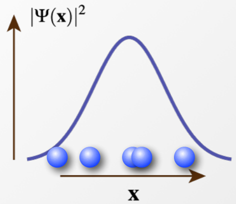

Single Particle

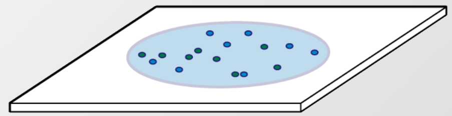

Correlated 2D Quantum Liquid

$\Psi(\mathbf{x})$	wave function	$\Psi(\mathbf{x}_1, \mathbf{x}_2, \mathbf{x}_3, \ldots, \mathbf{x}_N)$
$\|\Psi(\mathbf{x})\|^2$	probability distribution	$\|\Psi(\mathbf{x}_1, \mathbf{x}_2, \mathbf{x}_3, \ldots, \mathbf{x}_N)\|^2$

averaging over single-particle measurements, we obtain $|\Psi(\mathbf{x})|^2$

For many-body system: need access to single snapshots of the many-particle system!

Enables Measurement of Non-local Correlations

Single Atoms — Measuring a Many-Body Quantum System

Local occupation measurement

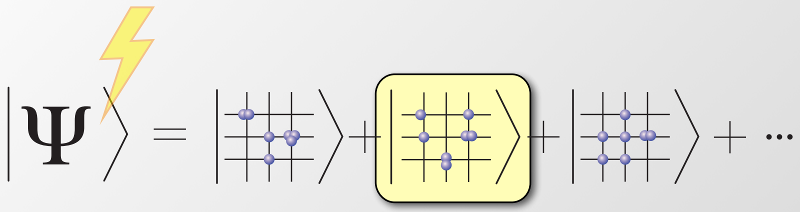

Enables access to all position correlation between particles!

Extendable to other observables (e.g. local currents etc…)

Single Atoms — Experimental Setup

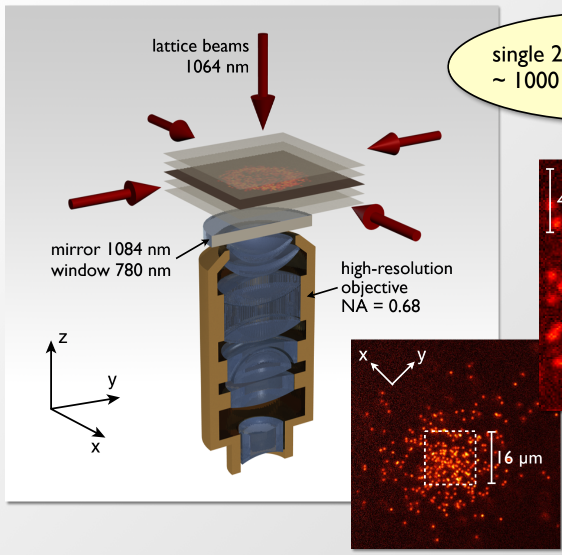

single 2D degenerate gas ~ 1000 ^{87}Rb atoms (bosons)

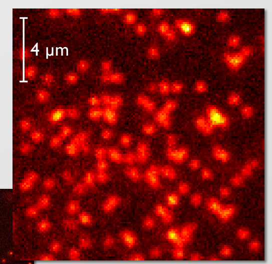

resolution of the imaging system: ~700 nm

LMU

Snapshot of an Atomic Density Distribution

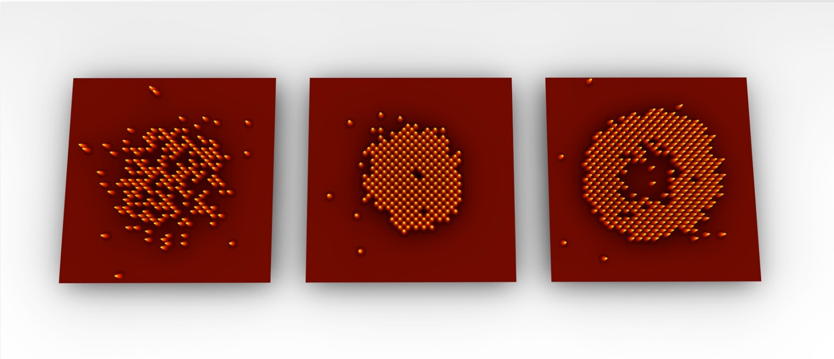

BEC

n=1
Mott Insulator

n=1 & n=2
Mott Insulator

J. Sherson *et al.* Nature **467**, 68 (2010); see also: W. Bakr *et al.* Science **329**, 547 (2010)

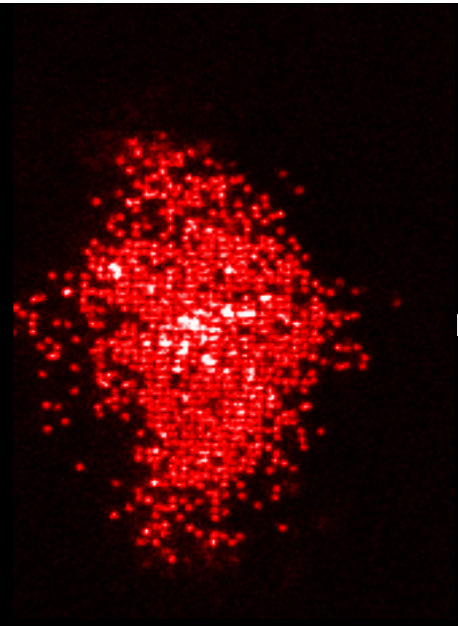

Now also for fermions

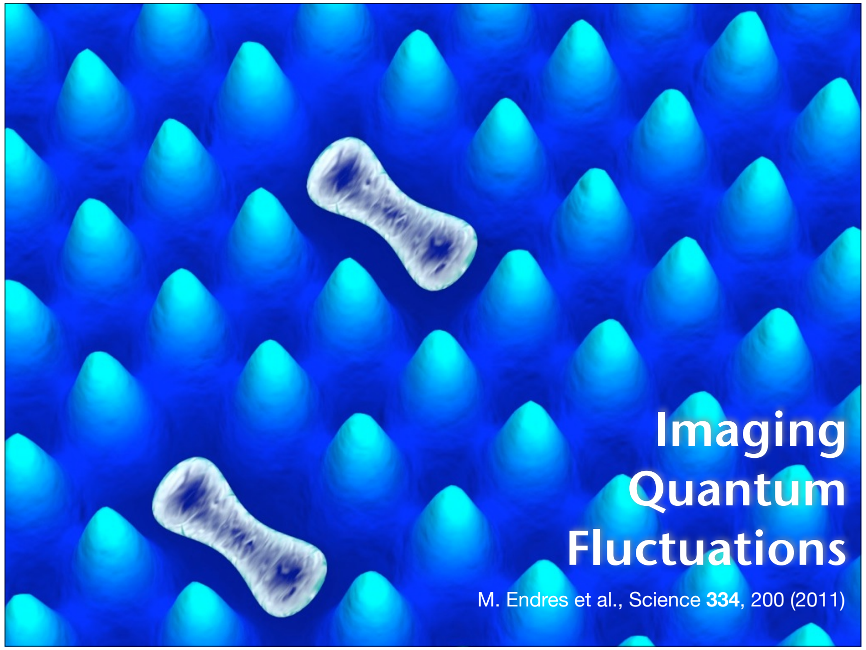

Realizing Artificial Gauge Fields in Optical Lattices

Artificial Gauge Fields

1) Rotation

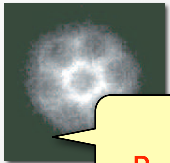

In rapidly rotating gases, ***Coriolis force*** is equivalent to ***Lorentz force***.

v × rot

al., PRL (2000)
Science (2001)

Problem in both cases: small B-fields (large ν>1000 for now), heating...

2) Raman

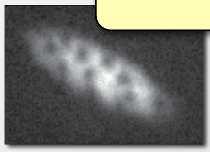

Spatially dependent optical couplings lead to a **Berry phase** analoguous to the **Aharonov-Bohm phase**

Y. Lin *et al.*, Nature (2009)

Artificial B-Fields with Ultracold Atoms

Controlling atom tunneling along *x* with Raman lasers leads to effective tunnel coupling with spatially-dependent Peierls phase ( )

h.c.

ough a plaquette:

$S = \varphi_1 - \varphi_2$

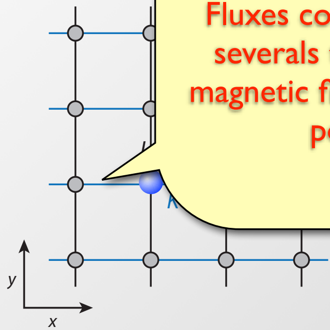

Fluxes corresponding to severals thousand Tesla magnetic field strength are possible!

h & P. Zoller, New J. Phys. (2003)
& J. Dalibard, New J. Phys. (2010)
N. Cooper, PRL (2011)
E. Mueller, Phys. Rev. A (2004)
L.-K. Lim et al. Phys. Rev. A (2010)
A. Kolovsky, Europhys. Lett. (2011)

see also: lattice shaking
E. Arimondo, PRL(2007) , K. Sengstock, Science (2011),
M. Rechtsman & M. Segev, Nature (2013), T. Esslinger Nature (2014)

Harper Hamiltonian and Hofstadter Butterfly

Harper Hamiltonian: *J*=*K* and ϕ uniform.

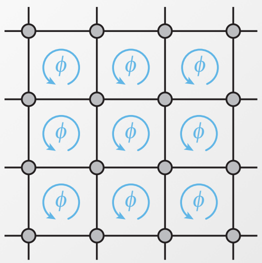

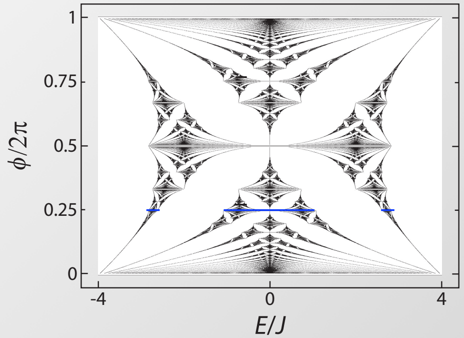

The lowest band is topologically equivalent to the lowest Landau level.

D.R. Hofstadter, Phys. Rev. B**14**, 2239 (1976)
see alo Y. Avron, D. Osadchy, R. Seiler, Physics Today 38, 2003

Hamiltonian

Realization of the Hofstadter-Harper Hamiltonian

$$\hat{H} = -\sum_{m,n}\left(K e^{i\phi_{m,n}}\hat{a}^\dagger_{m+1,n}\hat{a}_{m,n} + J\hat{a}^\dagger_{m,n+1}\hat{a}_{m,n}\right) + \text{h.c.}$$

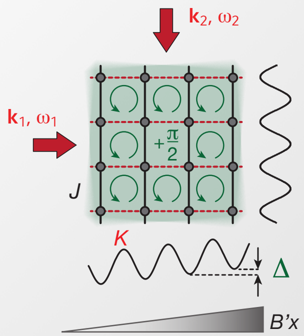

Scheme allows for the realization of an effective uniform flux of

$\Phi = \pi/2$

M. Aidelsburger *et al.*, PRL **111**, 185301 (2013)
H. Miyake *et al.*, PRL **111**, 185302 (2013)

Uniform Flux **Loading and Probing Hofstadter Bands**

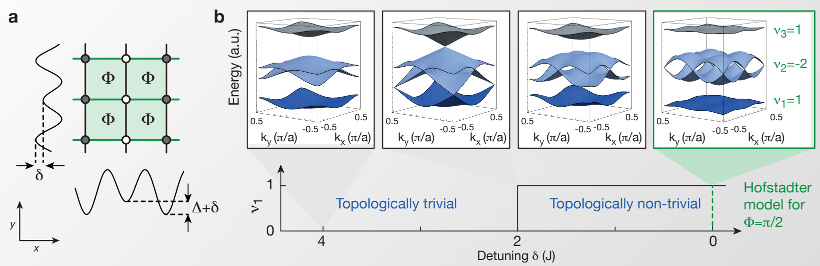

Key insight for adiabatic loading/probing:
keep Brillouin zone
of topologically trivial & non-trivial phase matched!

Flat bands realized! $gap/\ bw \simeq$

Uniform Flux **Hall Response & Anomalous Velocity**

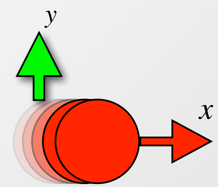

$$\hbar\frac{d\mathbf{k}}{dt} = -e\left(\nabla\phi(\mathbf{r}\ ) + \frac{d\mathbf{r}}{dt}\times\ (\mathbf{r}\ )\right)$$
$$\frac{d\mathbf{r}}{dt} = \frac{}{\hbar}\nabla_k\ _n(\mathbf{k_c}) - \frac{d\mathbf{k}}{dt}\times\ (\mathbf{k}\ )\hat{\mathbf{z}}$$

anomalous velocity

Karplus & Luttinger, Phys. Rev. (1954)
Sundaram & Niu, Phys. Rev. B (1999)

Uniform Flux **Cloud Deflection & Chern Number**

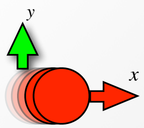

$$\mathbf{v}(\ ) = \frac{d\mathbf{r}}{dt} = \frac{}{\hbar}\nabla_k\ _n(\ ) - \frac{d}{dt}\times\ (\ )\hat{\mathbf{z}}$$

Assume uniformly filled band and rational flux p/q:

$$\langle v_x\rangle = \frac{}{N_{at}}\int \rho(\ )\, v_x(\ )\, d^2k$$
$$= -\frac{}{N_{at}}\cdot 2\pi\cdot\frac{N_{at}}{k_x\ \ k_y}\cdot\frac{y}{\hbar}\cdot\frac{}{2\pi}\int\ (\ )\,d^2k$$
$$= -(2\pi)^2\cdot\frac{}{(2\pi/a)(2\pi/qa)}\cdot\frac{y}{h}\cdot\nu$$
$$= -\frac{y\,qa^2}{h}\nu$$

H. Price & N. Cooper PRA (2012)
A. Dauphin & N. Goldman PRL (2013)

Uniform Flux **Chern Number Measurement**

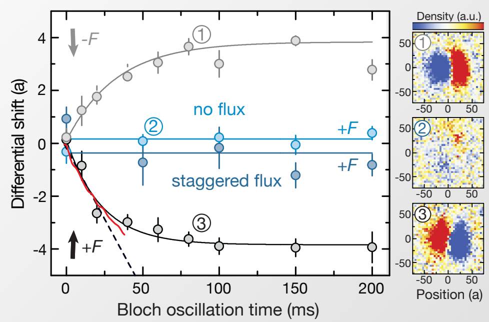

$$_{xp} = 0.99(\ )$$

Experimentally measured Chern number
(in agreement with linear fit to short time dynamics)

M.A. *et al.*, Nature Physics 11, 162 (2015)

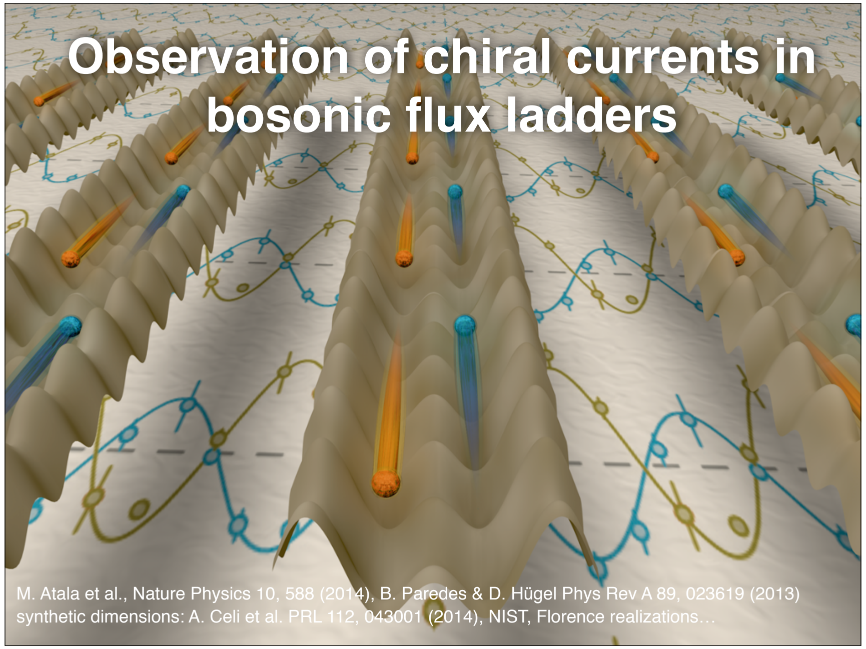

Flux ladder: experimental realization

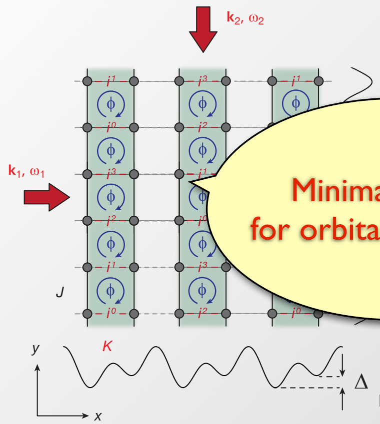

- resonant laser-assisted tunneling:

$$\omega_1 - \omega_2 = \Delta/\hbar$$

Minimal System for orbital magnetism

…dent phase factors

$\cdot\ \pi/2$

…ux

$$\Phi = \pi/2$$

Experiment: M. Atala et al., Nature Physics 10, 588 (2014)
Theory: D. Hügel, B. Paredes, PRA 89, 023619 (2014)
E. Orignac & T. Giamarchi PRB 64, 144515 (2001)
A. Tokuno & A. Georges New J. Phys. 16, 073005 (2014)
R. Wei & E. Mueller PRA 89, 063617 (2014)
M. Piraud, F. Heidrich-Meisner, et al. Phys. Rev. B 91, 140406(R) (2015)

Flux Ladder Hamiltonian

Hamiltonian of the system written in a simpler theory gauge

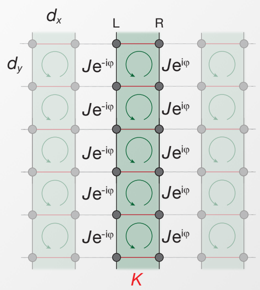

$$H = -J\sum_\ell \left(e^{-i\ell\varphi}\hat{a}^\dagger_{\ell+1;L}\hat{a}_{\ell;L} + e^{i\ell\varphi}\hat{a}^\dagger_{\ell+1;R}\hat{a}_{\ell;R}\right) - K\sum_\ell \left(\hat{a}^\dagger_{\ell;L}\hat{a}_{\ell;R}\right) + \text{h.c.}$$

Flux: $\phi = 2\varphi$

Define: $\hat{a}_{q;\mu} = \sum_\ell e^{iq\ell}\hat{a}_{\ell;\mu},$

and solve for the ansatz $|\psi_q\rangle = (\alpha_q \hat{a}^\dagger_{q;L} + \beta_q \hat{a}^\dagger_{q;R})\,|0\rangle$

Ladder Band Structure

Two energy bands

$$\epsilon_q = 2J\cos(q)\cos(\varphi) \pm \sqrt{K^2 - 4J^2\sin^2(\varphi)\sin^2(q)}$$

$\phi = 2\varphi = \pi/2$

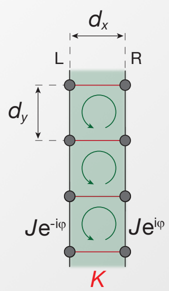

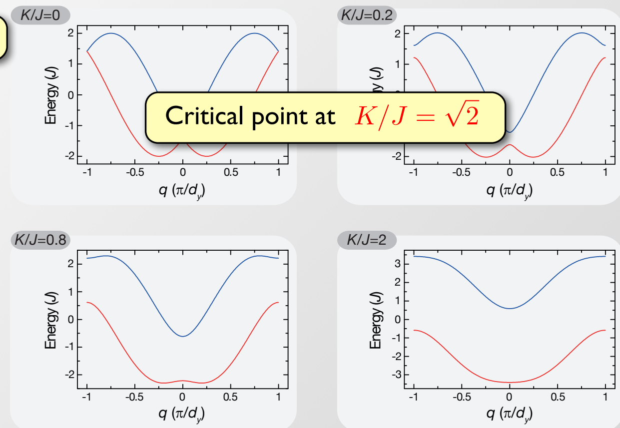

Critical point at $K/J = \sqrt{2}$

Probability Currents in Ladder

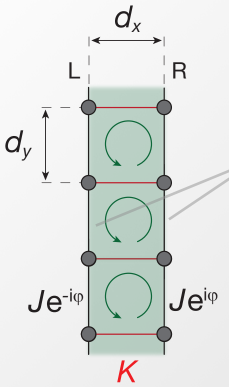

Current along the legs:

$$\hat{\mathbf{j}}^y_{\ell;\mu} = -\frac{i}{\hbar}\left(\hat{a}^\dagger_{\ell+1;\mu}\hat{a}_{\ell;\mu}H_{\ell\to\ell+1;\mu} - \text{h.c}\right)$$

$\mu = $ (L=left,R=right)

In the experiment ***total current*** is measured

$$\mathbf{j} = N^{-}_{leg} \sum_{l} \mathbf{j}^y_{l;}$$

Chiral current: $\mathbf{j} = \mathbf{j}_{\mathrm{L}} - \mathbf{j}_{\mathrm{R}}$

Phase Diagram

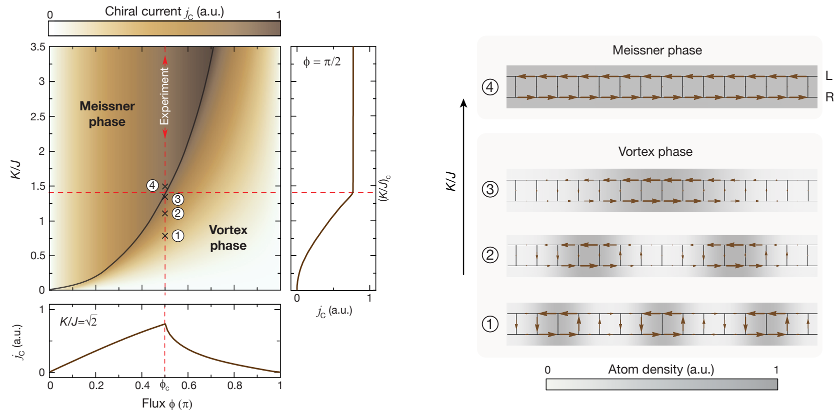

see E. Orignac & T. Giamarchi PRB 64, 144515 (2001)

Spin-orbit coupling - short digression

- The flux ladder Hamiltonian can be mapped into a spin-orbit coupled system
- Left right legs are mapped into pseudo-spins:

$$\hat{a}_{\ell;R} \to \hat{a}_{\ell;\downarrow} \qquad \hat{a}_{\ell;L} \to \hat{a}_{\ell;\uparrow}$$

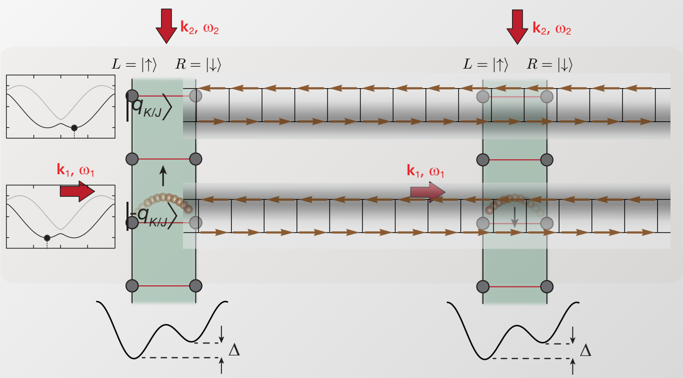

Spin-Momentum locking: D. Hügel, B. Paredes, PRA 89, 023619 (2014)
Continuum: I. B. Spielman Nature 471, 83 (2011)

Current Measurements: Sequence

How to measure currents in our setup?

→ *project the state into isolated double wells*

S. Trotzky *et al.* Nature Physics 8, 325 (2012)
S. Kessler & F. Marquardt, arXiv:1309.3890 (2012)

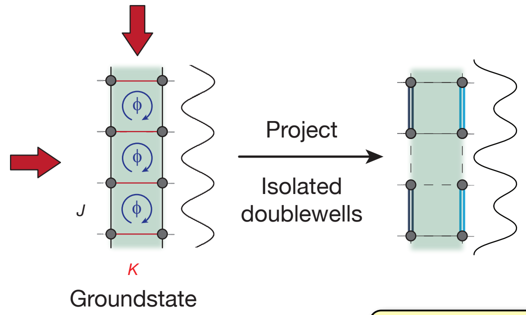

- Hold in double wells for a time t
- Measure *even-odd population* in double well

Josephson oscillations in double wells

Double well oscillations - currents

In the experiment we measure the average of all the oscillations on either side of the ladder:

$$n_{\text{even};\mu}(t) = \frac{1}{2}[1 + (n_{\text{even};\mu}(0) - n_{\text{odd};\mu}(0))\cos(2\omega t) - \frac{j_\mu}{J/\hbar}\sin(2\omega t)]$$

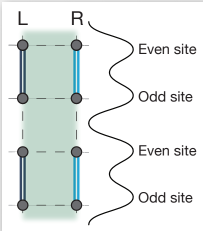

Oscillations in double wells

- Prepare ground state of the flux ladder with K/J=2 and project into isolated double wells

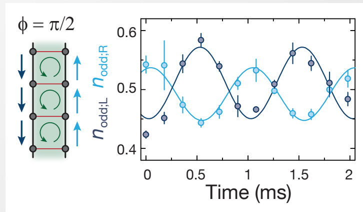

Reversed flux

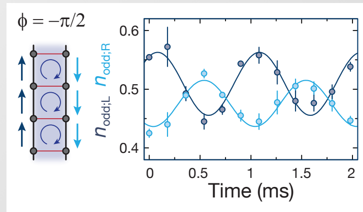

When inverting the flux the current gets reversed

Zero flux ladders

- Prepare ground state of the ladder with zero flux
- project into isolated double wells

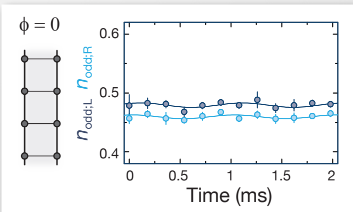

Extracting the Chiral current

The chiral current can be reliably calculated by

$$n_{\text{even};\mu}(t) = \frac{1}{2}[1 + (n_{\text{even};\mu}(0) - n_{\text{odd};\mu}(0))\cos(2\omega t) - \frac{j_\mu}{J/\hbar}\sin(2\omega t)]$$

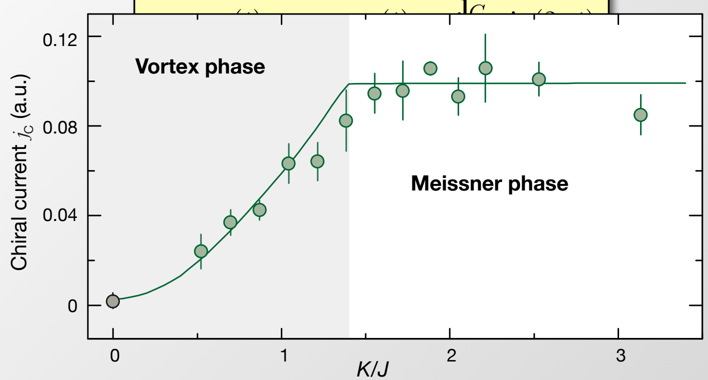

Summary and Outlook

- *New detection method* for probability currents
- Measurement of *Chiral Edge States* in Ladders (also possible locally!!)
- Identification of *Meissner-like effect in bosonic ladder*

Outlook:

- Entering the strongly correlated regime
- Chiral Mott Insulators
- Spin Meissner effect
- Connection of chiral ladder states to Hoftstadter model edge states
- Spin-Orbit Coupling in 1D

E. Orignac & T. Giamarchi PRB 64, 144515 (2001)
Dhar, A *et al.*, PRA 85, 041602 (2012)
Petrescu, A. & Le Hur, K. PRL 111, 150601 (2013)
A Tokuno & A Georges, NJP 16 , 073005 (2014)
R. Wei & E. Mueller PRA 89, 063617 (2014)
S. Greschner et al. arXiv:1504.06564 (2015)
M. Piraud, F. Heidrich-Meisner, et al. Phys. Rev. B 91, 140406(R) (2015)

Probing Band Topology

Measuring the Zak-Berry's Phase of Topological Bands

M. Atala et al., Nature Physics (2013)

www.quantum-munich.de

Berry Phase in Quantum Mechanics

$$\Psi(R) \rightarrow e^{i(\varphi_{\text{Berry}}+\varphi_{\text{dyn}})}\ \Psi(R)$$

Adiabatic evolution through closed loop

$$\varphi_{\text{Berry}} = \oint_{\mathcal{C}} A_n(R)dR = i\oint_{\mathcal{C}} \langle n(R)|\nabla_R|n(R)\rangle\, dR$$

$$\varphi_{\text{Berry}} = \oint_{\mathcal{A}} \Omega_n(R)\, dA$$

Berry Phase

M.V. Berry, Proc. R. Soc. A (1984)

Berry connection

$$A_n(R) = i\langle n(R)|\nabla_R|n(R)\rangle$$

Berry curvature

$$\Omega_{n,\mu\nu}(R) = \frac{\partial}{\partial R^\mu}A_{n,\nu} - \frac{\partial}{\partial R^\nu}A_{n,\mu}$$

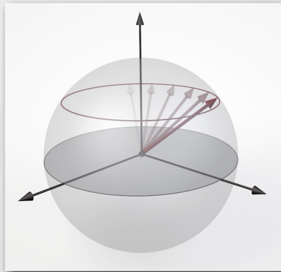

Example: Spin-1/2 particle in magnetic field

Berry Phase for Periodic Potentials

$\Psi_k(\mathbf{r}) = e^{i\mathbf{kr}} u_k(\mathbf{r})$ Bloch wave in periodic potential

Adiabatic motion in momentum space generates Berry phase!

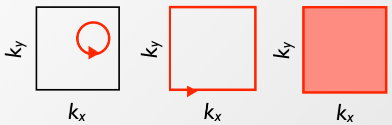

Berry phase is fundamental to characterize topology of energy bands

$$n_{\text{Chern}} = \frac{1}{2\pi}\oint_{BZ} A_k dk = \frac{1}{2\pi}\int_{BZ} \Omega_k \, d^2k \quad \Leftrightarrow \quad \sigma_{xy} = n_{\text{Chern}}\, e^2/h$$

Chern Number (Topological Invariant) **Quantized Hall Conductance**

Thouless, Kohmoto, den Nijs, and Nightingale (TKNN), PRL 1982
Kohmoto Ann. of Phys. 1985

What is the extension to 1D?

Mention Problem with going on a line is generally NOT A LOOP IN PARAMETER SPACE!

Zak Phase

2D Brillouin Zone

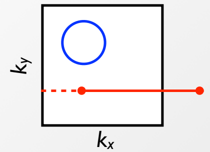

going straight means going around!

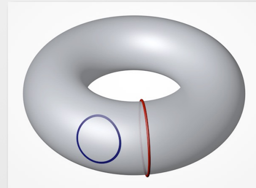

Band structure has torus topology!

$$\varphi_{Zak} = i\int_{k_0}^{k_0+G} \langle u_k|\partial_k|u_k\rangle \; dk$$

Zak Phase - the 1D Berry Phase
J. Zak, Phys. Rev. Lett. **62**, 2747 (1989)

Non-trivial Zak phase:

- Topological Band
- Edge States (for finite system)
- Domain walls with fractional quantum numbers

R. Jackiw and C. Rebbi, Phys. Rev. D 13, 3398 (1976)
J. Goldstone and F. Wilczek, Phys. Rev. Lett. 47, 986 (1981)

Su-Shrieffer-Heeger Model (SSH)

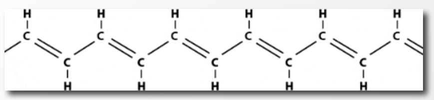

Polyacetylene
W. P. Su, J. R. Schrieffer & A. J. Heeger
Phys. Rev. Lett. 42, 1698 (1979).

$$SS \; = - \; \{J\hat{a}_n^\dagger\hat{b}_n + J'\hat{a}_n^\dagger\hat{b}_{n-1} + \text{h. .}\}$$
n

Two topologically distinct phases:

D1: $J > J'$

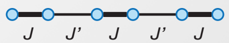

D2: $J' > J$

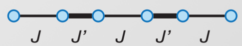

$$\delta\varphi_{Zak} = \varphi_{Zak}^{D1} - \varphi_{Zak}^{D2} = \pi$$

Topological properties:
domain wall features fractionalized excitations

Zak phase difference $\delta\varphi_{Zak}$ is gauge-invariant

SSH Energy Bands - Eigenstates

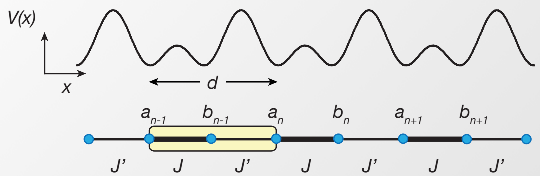

...ABABA... Lattice Structure....

$$\sum_x \Psi_x = \sum_x e^{ikx} \times \begin{cases} \alpha_k \\ \beta_k \; e^{ikd/2} \end{cases}$$

2x2 Hamiltonian:

$$\begin{bmatrix} 0 & -\rho_k \\ -\rho_k^* & 0 \end{bmatrix} \begin{pmatrix} \alpha_k \\ \beta_k \end{pmatrix} = \tilde{\epsilon}_k \begin{pmatrix} \alpha_k \\ \beta_k \end{pmatrix}$$

with $\rho_k = Je^{ikd/2} + J'e^{-ikd/2} = |\epsilon_k|e^{i\theta_k}$

SSH Energy Bands - Eigenstates

...ABABA... Lattice Structure....

$$\sum_x \Psi_x = \sum_x e^{ikx} \times \begin{cases} \alpha_k \\ \beta_k \ e^{ikd/2} \end{cases}$$

Eigenstates

$$\begin{pmatrix} \alpha_{k,\mp} \\ \beta_{k,\mp} \end{pmatrix} = \frac{1}{\sqrt{2}} \begin{pmatrix} \pm 1 \\ e^{-i\theta_k} \end{pmatrix}$$

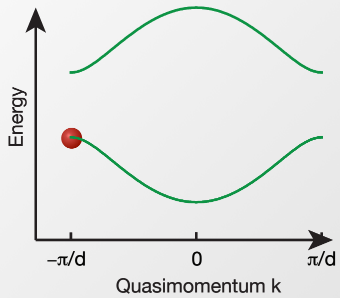

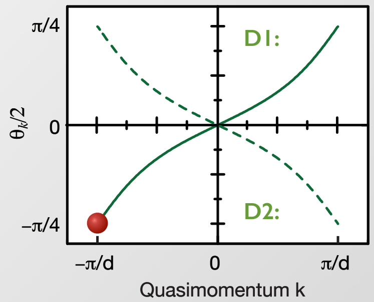

D1: $J \geq J'$ $\varphi_{Zak} = i \int_{k_0}^{k} \ldots$ $\varphi^{D1}_{Zak} = \frac{\pi}{2}$ $\frac{1}{2} \int_{k_0}^{G+k_0}$ D2: $J' > J$ $\partial_k \theta_k$ $\varphi^{D2}_{Zak} = -\frac{\pi}{2}$

Adiabatic evolution in momentum space

Realization with ultracold atoms

$$_{ss} = - \sum_n \{J a_n^\dagger b_n + J' a_n^\dagger b_{n-1} + \text{h.c.}\}$$

767 nm
1534 nm

D1: $J > J'$ D2: $J' > J$

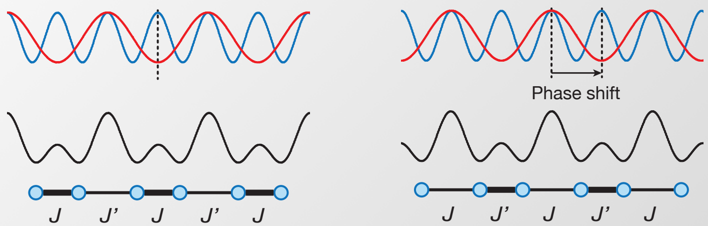

$$\delta\varphi_{Zak} = \varphi^{D1}_{Zak} - \varphi^{D2}_{Zak} = \pi$$

Measuring the Berry-Zak Phase (SSH Model)

D1: $J > J'$ Spin-dependent Bloch oscillations + Ramsey interferometry

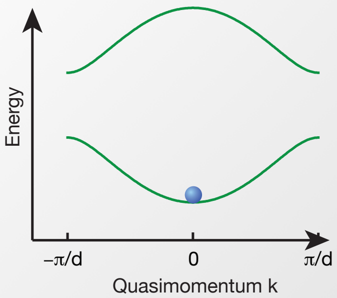

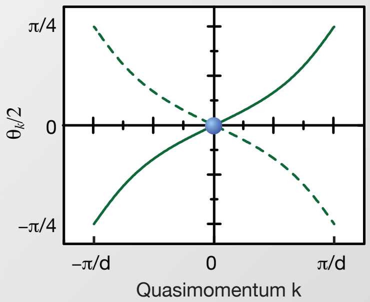

Prepare BEC in state $|\sigma, k\rangle = |\downarrow, 0\rangle$, with $\sigma = \uparrow, \downarrow$

Measuring the Berry-Zak Phase (SSH Model)

D1: $J > J'$

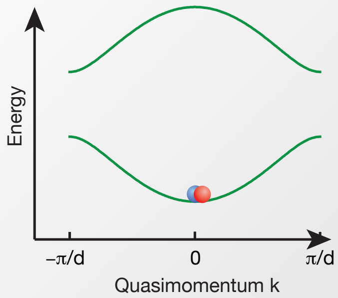

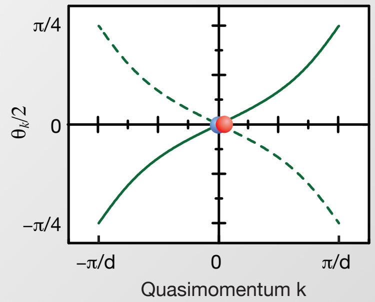

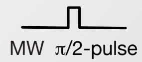

Spin components with opposite magnetic moments!

Create coherent superposition $\frac{1}{\sqrt{2}} (|\uparrow, 0\rangle + |\downarrow, 0\rangle)$

Measuring the Berry-Zak Phase (SSH Model)

DI: $J > J'$

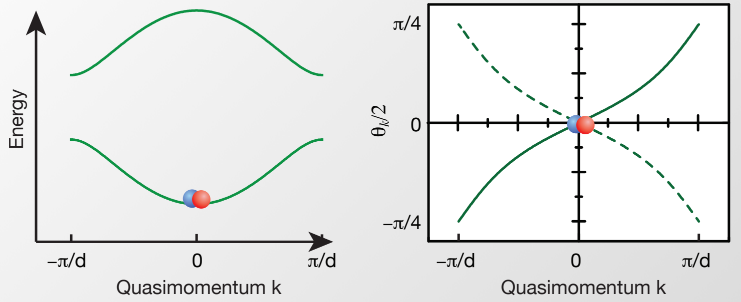

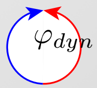

$\varphi_{dyn} = \int E(t)/\hbar \, dt$

Closed Loop in k-Space

$E(k) = E(-k)$

c evolution in momentum space

$$\delta\varphi_{Zak} = \varphi_{Zak}^{D1} + \varphi_{dyn} + \varphi_{Zeeman}$$

(with φ_{dyn} crossed out)

Reference measurement

Phase of reference fringe:

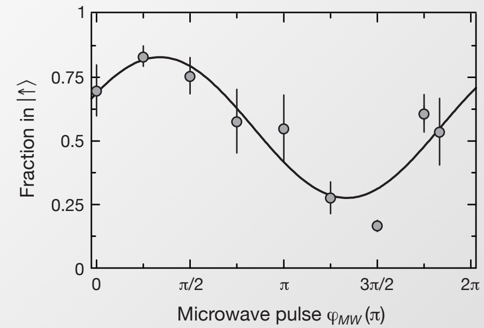

$$\delta\varphi \neq 0$$

Average of five individual measurements

Exp. imperfections:
- Small detuning of the MW-pulse
- Magnetic field drifts

Measuring the Zak Phase (SSH Model)

Measured Topological invariant:
Zak phase difference

$$\varphi_{Zak}^{D1} - \varphi_{Zak}^{D2} = \pi$$

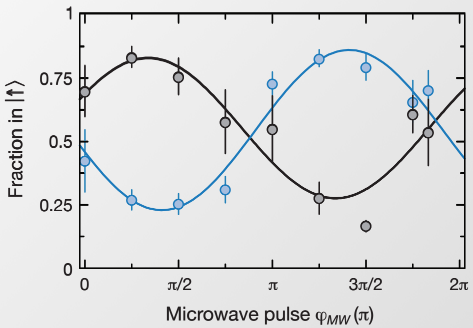

$$\delta\varphi_{Zak} = 0.97(2)\pi$$

obtained from 14 independent measurements

Measuring the Zak Phase (SSH Model)

Measured Topological invariant:
Zak phase difference

$$\varphi_{Zak}^{D1} - \varphi_{Zak}^{D2} = \pi$$

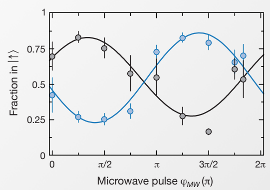

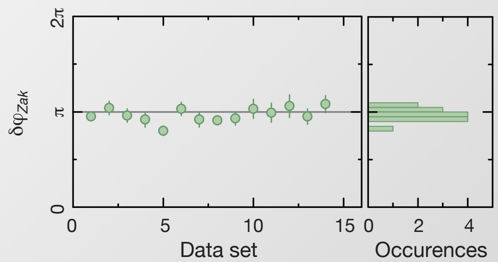

$$\delta\varphi_{Zak} = 0.97(2)\pi$$

obtained from 14 independent measurements

Geometric Phase

Fractional Zak Phase

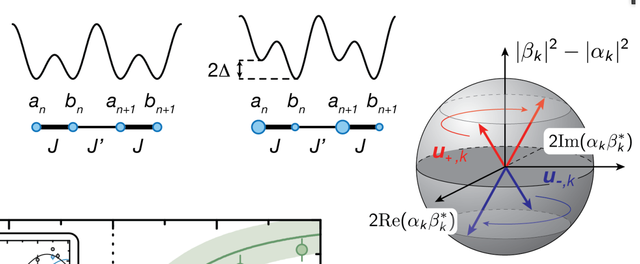

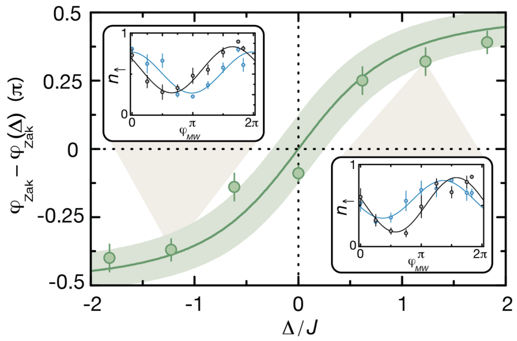

Zak Phase becomes **fractional** for heteropolar dimerization!

SSH

Measuring Fractional Charge

Probability Density of Eigenstates

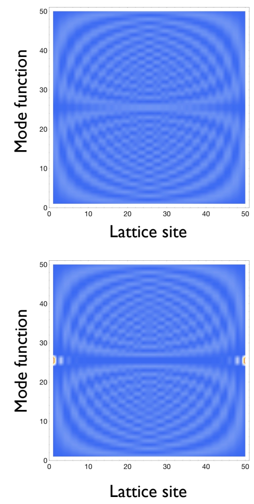

Lattice Topology

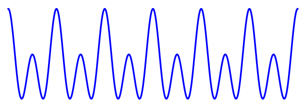

Topologically Trivial

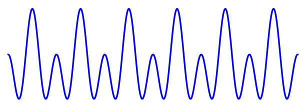

Topologically Non-Trivial

SSH

Fractional Charge

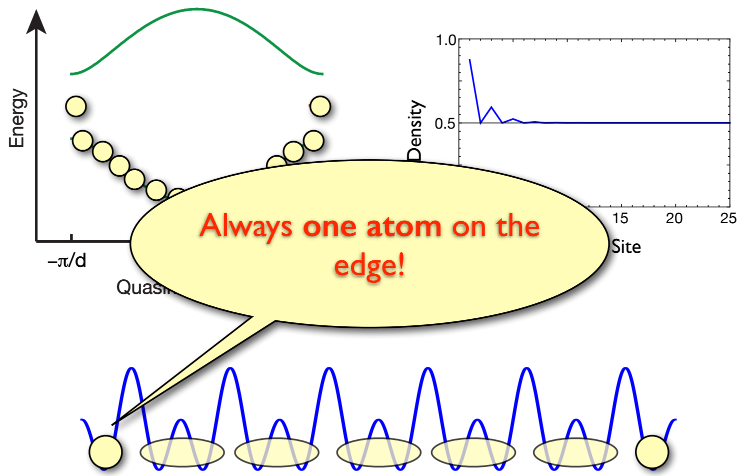

R. Rajaraman & J. Bell, Phys. Lett B 1982, Nucl. Phys. B 1983

An Aharonov Bohm Interferometer for Determining Bloch Band Topology

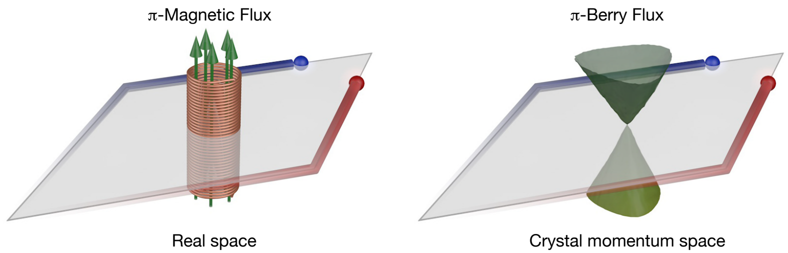

D. Abanin E. Demler

L. Duca et al. Science **347**, 288 (2015)
D. Abanin et al. PRL **110**, 165304 (2013)

AB

Aharonov-Bohm Effect

Real Space

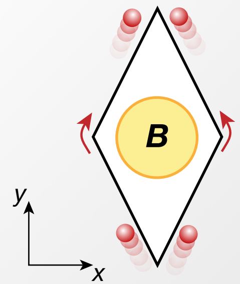

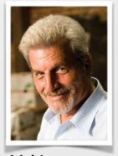

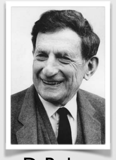

..., contrary to the conclusions of classical mechanics, there exist effects of potentials on charged particles, even in the region where all the fields (and therefore the forces on the particles) vanish.

$$_B = \frac{q}{\hbar}\oint_C (\mathbf{r})\, d\mathbf{r} = \frac{q}{\hbar}\int_S \times (\mathbf{r})\, d\ r$$

$$_B = \frac{q}{\hbar}\int dS = \pi / _0$$

Aharonov-Bohm Phase

Y. Aharonov & D. Bohm Phys. Rev.(1959)
W. Ehrenberg & R. Siday Proc. Phys. Soc B (1949)
Exp: A. Tonomura, et al. Phys. Rev. Lett. (1986)

Geometry

Illustrating Geometric Phases

Parallel transport on a surface

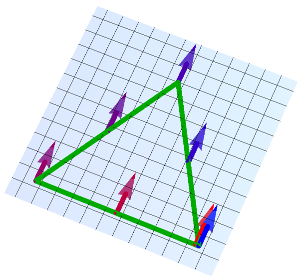

Flat manifold: $\varphi_G = 0$

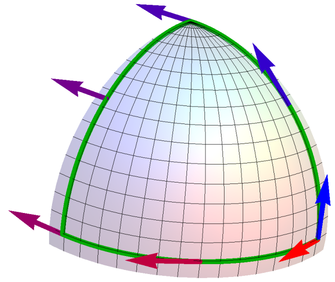

Curved manifold: $\varphi_G \neq 0$

measures the **integrated Gaussian curvature** enclosed by chosen path

Band Topology

Hexagonal Lattices

__Lattice:__ A and B degenerate sublattices

$$= _0 - J \sum_{i=1}^{3} \left(\hat{a} \ \hat{b}^\dagger_{+\mathbf{d}_i} + \mathrm{h.\ c.}\right)$$

Real Space

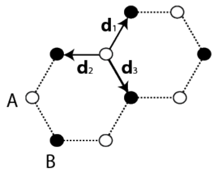

__Lowest energy bands:__

Dirac points at the corners of the first BZ

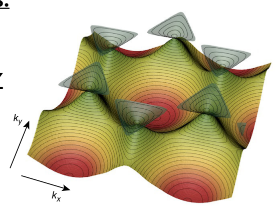

Reciprocal Space

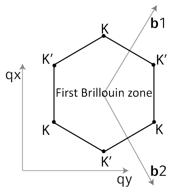

A. Castro Neto et al., Rev. Mod. Phys. **81**, 109 (2009)
__cold atoms:__ hexagonal - K. Sengstock (Hamburg), brick wall - T. Esslinger (Zürich)

Band Topology — Scalar & Geometric Features

Band structure characterized by **scalar** & **geometric** features!

Eigenstates: Bloch waves $_{,n}(\mathbf{r}) = {}^{i\ \mathbf{r}} u\ _{,n}(\mathbf{r})$

Scalar Features

Dispersion relation

$_{,n}$

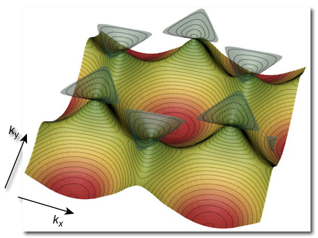

Geometric Features

Berry connection

$_n(\mathbf{q}) = \langle u_{\mathbf{q},n}|\ \ _{\mathbf{q}}|u_{\mathbf{q},n}\rangle$

Berry curvature

$(\mathbf{q}) = \nabla_{\mathbf{q}} \times\ \ _{\mathbf{n}}(\mathbf{q}) \cdot \mathbf{e}_z$

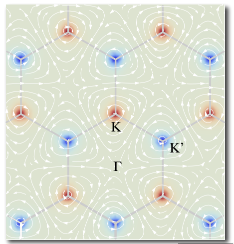

Stückelberg — Accelerating the Lattice

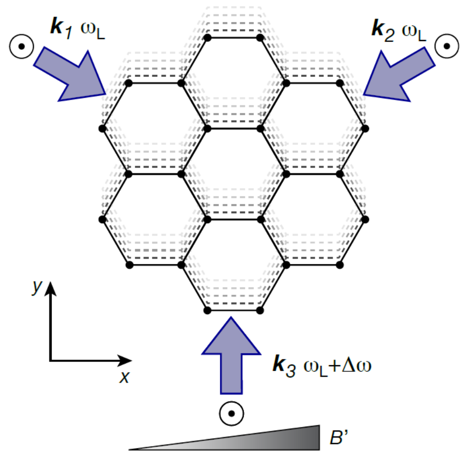

Arbitrary accelerations in any direction can be applied!

Stückelberg — Bloch Oscillations

Bloch oscillations induced by accelerating the lattice

weaker force

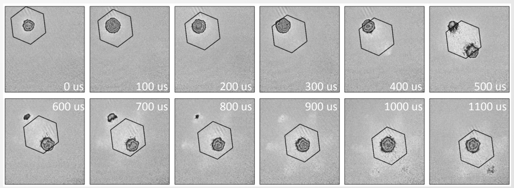

quasi-momentum distribution

stronger force

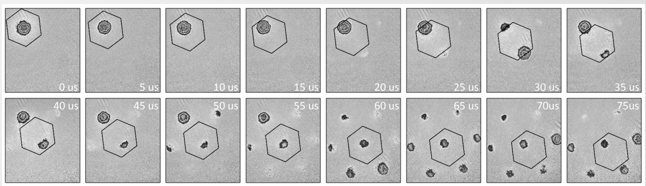

Band Topolgy — 'Aharonov Bohm' Interferometer in Momentum Space

Real Space

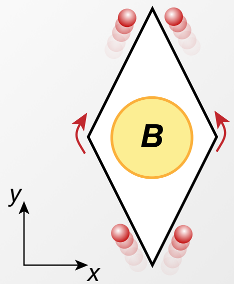

$_B = \frac{q}{\hbar}\oint_C\ \ (\mathbf{r})\, d\mathbf{r} = \frac{q}{\hbar}\int_S\ \ \times\ \ (\mathbf{r})\ d\ \ r$

$_B = \frac{q}{\hbar}\int\ \ d\mathbf{S} =\ \ \pi\ \ /\ \ _0$

Aharonov-Bohm Phase

Momentum Space

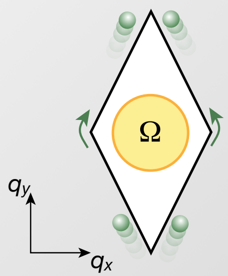

$_{\text{erry}} = \oint\ \ _n(\mathbf{q})\, d\mathbf{q} = \int_{S_q}\ \ \times\ \ _n(\mathbf{r})\ d\mathbf{S}_q$

$_{\text{erry}} = \int\ \ _n(\mathbf{q})\ \ \ _q$

Berry Phase

Band Topology — Berry Curvature in Hexagonal Lattices

Berry curvature concentrated to Dirac cones, alternating in sign!

Breaking time reversal or inversion symmetry gaps Dirac cones
and spreads Berry curvature out

Hexagonal Lattice Hamiltonian

$$(\ ) = \begin{pmatrix} & f(\ ) \\ f(\ ) & - \end{pmatrix}$$

Expanding momenta close to K Dirac point

$$(\tilde{\ }) = \begin{pmatrix} & \tilde{q}_x + i\tilde{q}_y \\ \tilde{q}_x - i\tilde{q}_y & \end{pmatrix}$$

Eigenstates

$$u^{\pm}_{,\tilde{\mathbf{q}}} = \frac{}{2}\begin{pmatrix} i \ (\mathbf{q})/2 \pm \ -i \ (\mathbf{q})/2 \end{pmatrix}$$

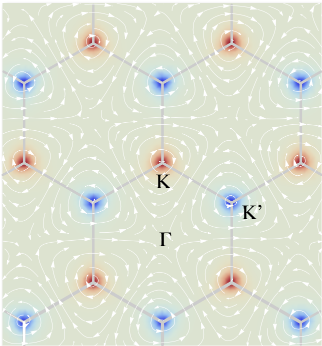

Band Topology — Berry Phases in Graphene

Berry Phase around K-Dirac cone

$$\text{erry},\mathbf{K} = \oint \ (\mathbf{q})\, d\mathbf{q} = \pi$$

Berry Phase around K'-Dirac cone

$$\text{erry}, \ ' = -\pi$$

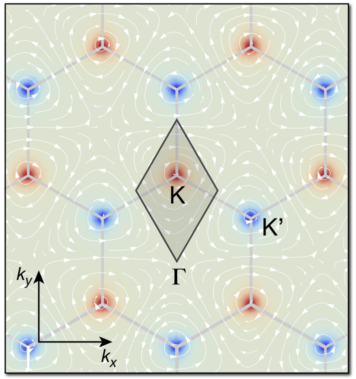

Stückelberg — Accelerating the Lattice

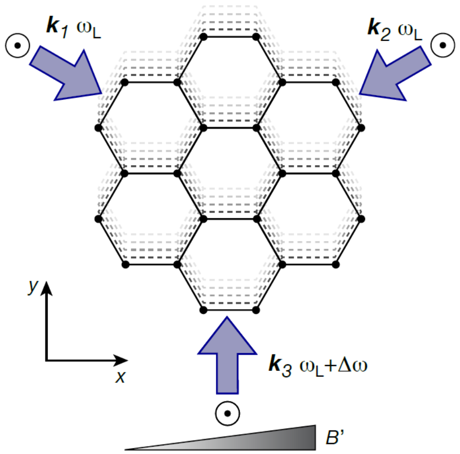

Arbitrary accelerations in any direction can be applied!

Stückelberg — Bloch Oscillations

Bloch oscillations induced by accelerating the lattice

weaker force

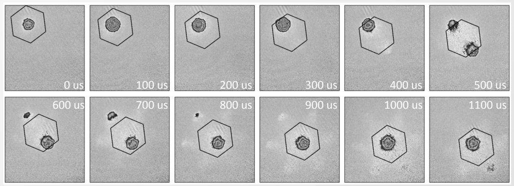

quasi-momentum distribution

stronger force

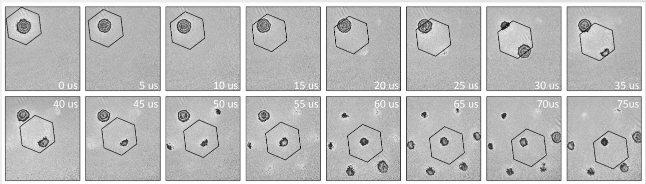

The Interferometer

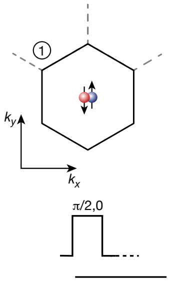

Forces applied by **lattice acceleration** and **magnetic gradients!**

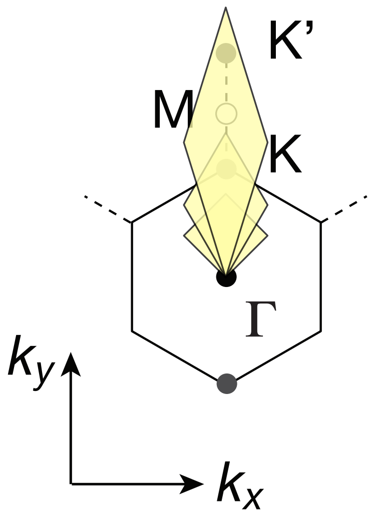

Interferometry Results

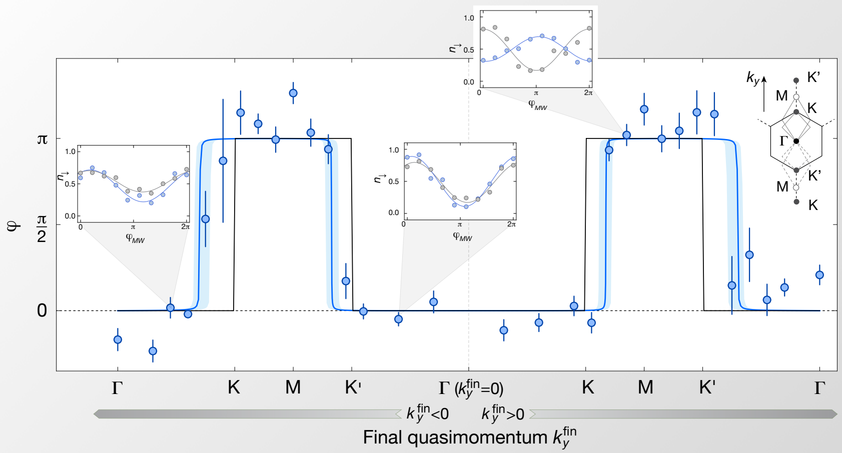

Zooming into the Edge

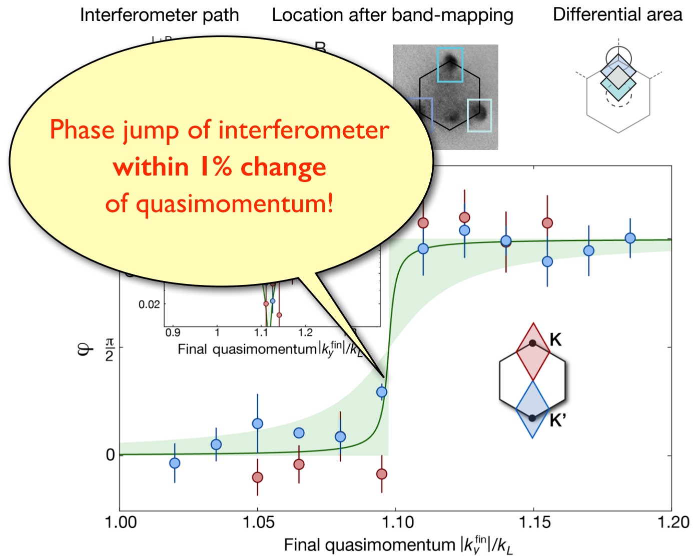

Changing Topology

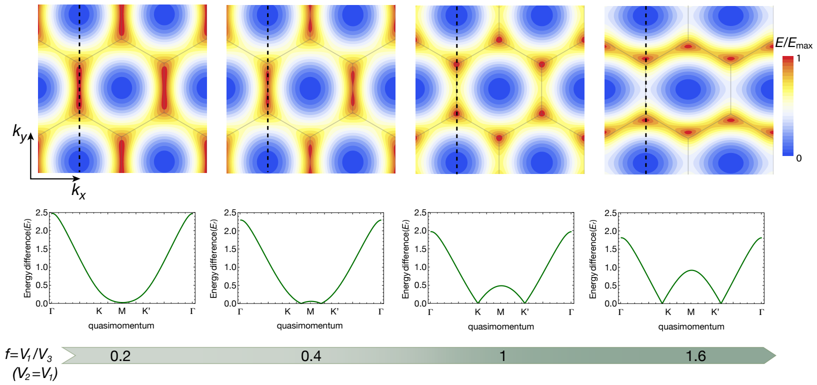

As long as T and I symmetry are preserved, Dirac cones are protected!

Robust Berry Flux at Dirac Cone

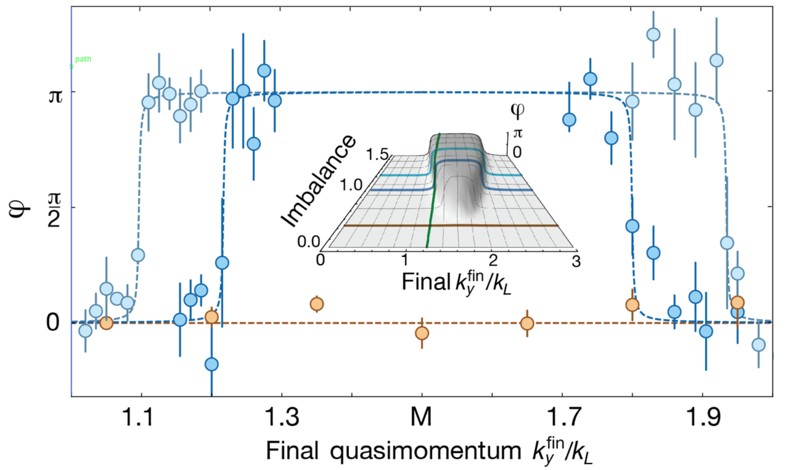

Interferometer Performance

Berry curvature spread $< 6 \times\ 0^{-4}$

pi-flux localized to 10^{-6} of Brillouin zone

A-B site offset $< h \times 12\ \ z$

Energy gap/Band width $3 \times\ 0^{-3}$

Multiple Bands
Stückelberg to Wilson Lines

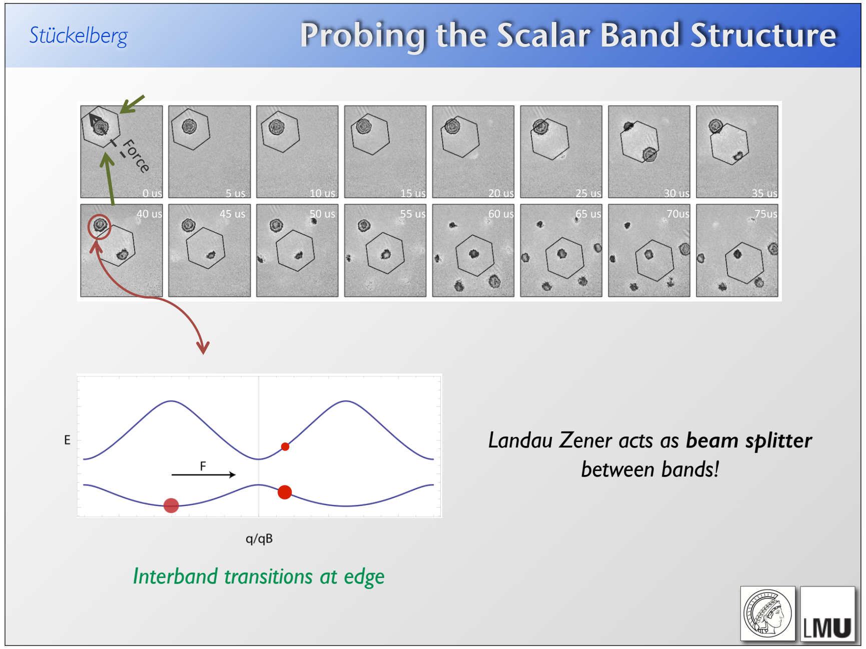
Stückelberg
Probing the Scalar Band Structure
Force
0 us
5 us
10 us
15 us
20 us
25 us
30 us
35 us
40 us
45 us
50 us
55 us
60 us
65 us
70us
75us
E
F
q/qB
Landau Zener acts as beam splitter between bands!
Interband transitions at edge
LMU

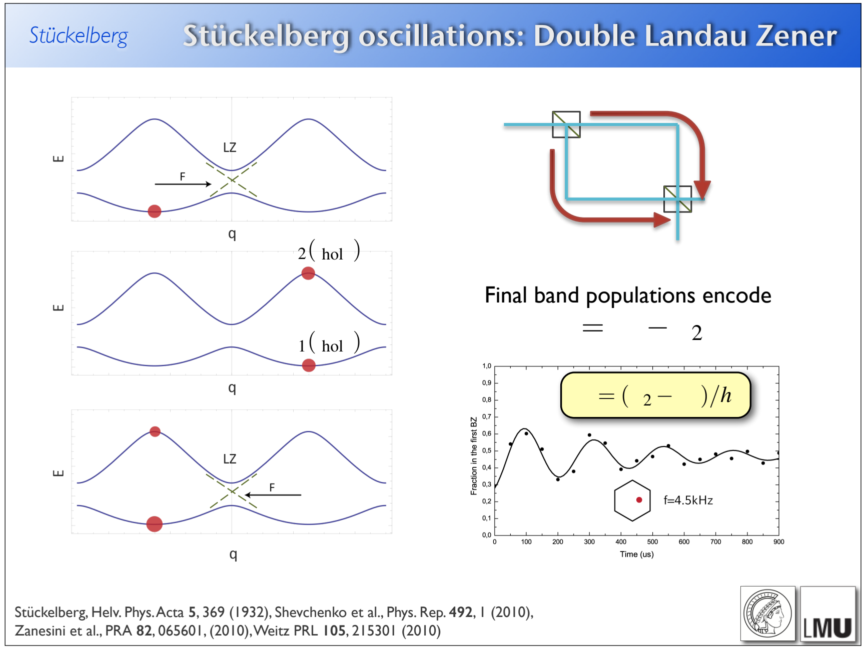
Stückelberg
Stückelberg oscillations: Double Landau Zener
E
LZ
F
q
Final band populations encode
f=4.5kHz
Time (us)
Stückelberg, Helv. Phys. Acta 5, 369 (1932), Shevchenko et al., Phys. Rep. 492, 1 (2010),
Zanesini et al., PRA 82, 065601, (2010), Weitz PRL 105, 215301 (2010)
LMU

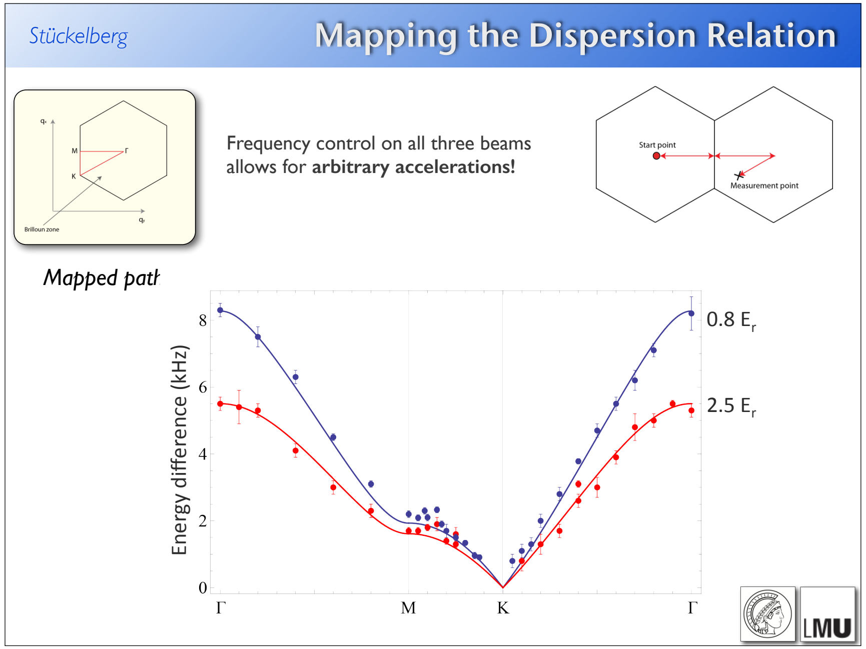
Stückelberg
Mapping the Dispersion Relation
Frequency control on all three beams allows for arbitrary accelerations!
Start point
Measurement point
Mapped path
Energy difference (kHz)
0.8 E_r
2.5 E_r
Γ
M
K
Γ
LMU

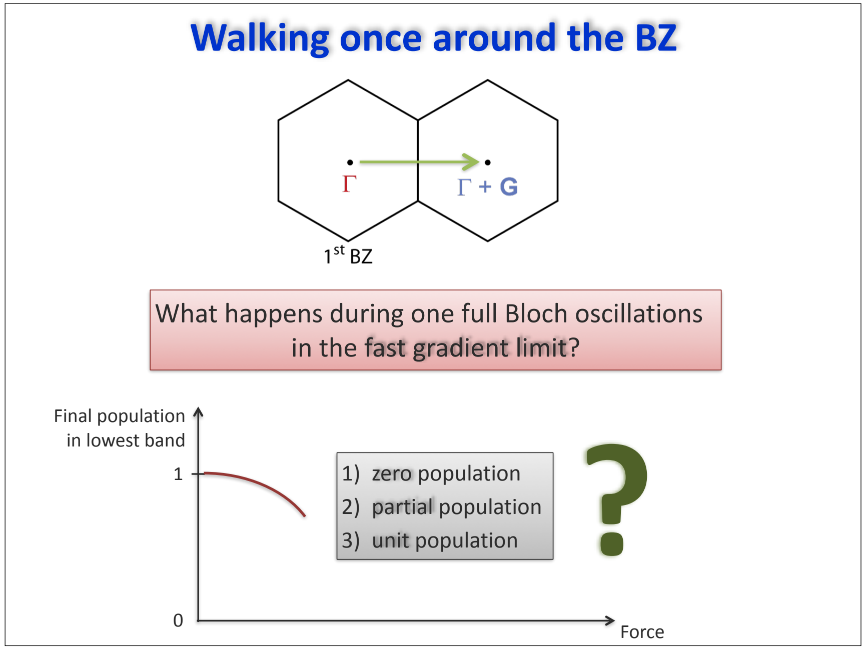
Walking once around the BZ
Γ
Γ + G
1st BZ
What happens during one full Bloch oscillations in the fast gradient limit?
Final population in lowest band
1
0
Force
1) zero population
2) partial population
3) unit population
?

Walking once around the BZ

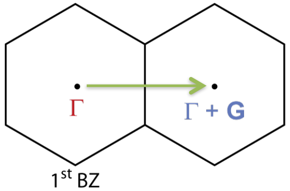

What happens during one full Bloch oscillations in the fast gradient limit?

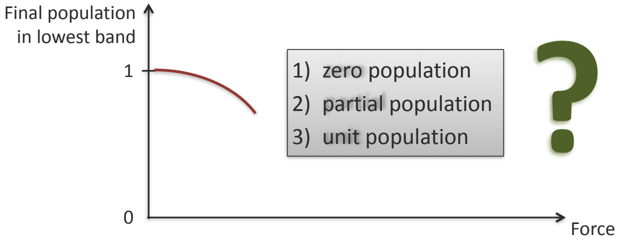

1) zero population
2) partial population
3) unit population

?

Excitation probability

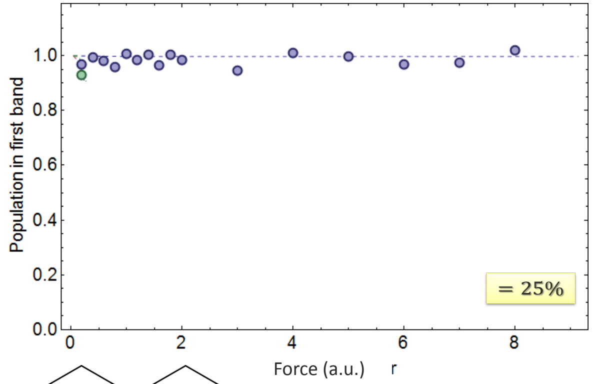

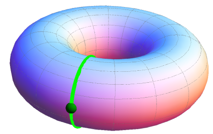

Non-contractable Path: Topologically discstinct from identy

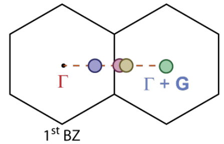

Wilson Lines

Multi-Band Geometry

Single Band

$$\mathbf{A}^n_{\mathbf{q}} = i\,\langle u^n_{\mathbf{q}}|\,\nabla_q\,|u^n_{\mathbf{q}}\rangle$$

Berry connection

$$\varphi_{AB} = \oint \mathbf{A}^n_{\mathbf{q}}\,d\mathbf{q}$$

Berry phase

$$U = \exp\left[i\varphi_{AB}\right]$$

U(1) unitary

φ_{AB} Gauge invariant

Multi-Band

$$\mathbf{A}^{n,n'}_{\mathbf{q}} = i\,\langle u^n_{\mathbf{q}}|\,\nabla_q\,|u^{n'}_{\mathbf{q}}\rangle$$

Non-abelian Berry conenction

$$\hat{\mathbf{U}}^{n,n'} = \mathcal{P}\ \ \mathrm{xp}[-i\oint \hat{\mathbf{A}}^{n,n'}_{\mathbf{q}}\,d\mathbf{q}]$$

U(n) Wilson loop

Wilczek & Zee PRL (1984)

Final population in fast gradient limit

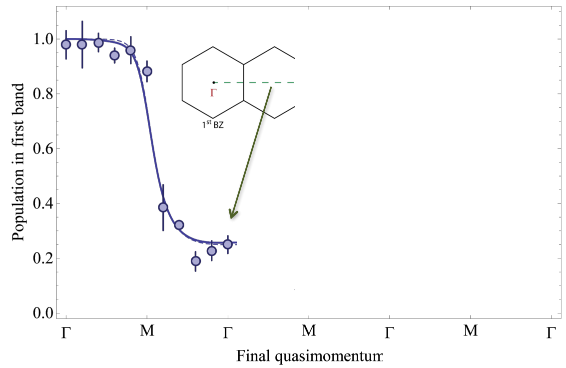

Dashed line: two band calculation

Solid line: Six bands

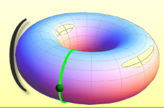

$$\left(\ \cdot\ \right)^3 \propto \begin{pmatrix} e^{i\varphi_1} & 0 \\ 0 & e^{i\varphi_2} \end{pmatrix}$$

Wilson-Zak Loops

Full characterization of two-band geometry
→ Reconstruct U(2) Wilson Loop

$$U(\Gamma\to\Gamma) = e^{i\varphi}\begin{pmatrix}\cos\left(\frac{2\pi}{3}\right)e^{i\alpha} & -\sin\left(\frac{2\pi}{3}\right)e^{i\beta}\\ \sin\left(\frac{2\pi}{3}\right)e^{-i\beta} & \cos\left(\frac{2\pi}{3}\right)e^{i\alpha}\end{pmatrix}$$

$$U(\Gamma\to\Gamma)^3 = \begin{pmatrix}e^{i\varphi_1} & 0\\ 0 & e^{i\varphi_2}\end{pmatrix}$$

φ, α available from Stückelberg & AB Interferometry (not shown)

Wilczek & Zee PRL (1984)

Real Space Interpretation

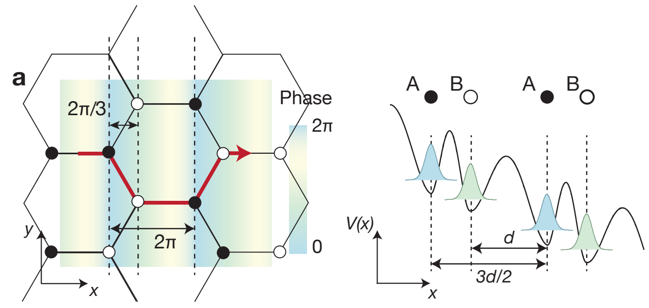

Geometric features depend on real space embedding of lattice!!

Thanks Gil!

Outlook

- Rectified Flux, Hofstadter Butterfly
- Novel Correlated Phases in Strong Fields, Transport Measurements
- Adiabatic loading schemes
- Spectroscopy of Hoftstadter bands
- Novel Topological Insulators
- Image Edge States - directly/spectroscopically
- Measure spatially resolved full current distribution
- Non-equilibrium dynamics in gauge fields
- Thermalization?

⋮

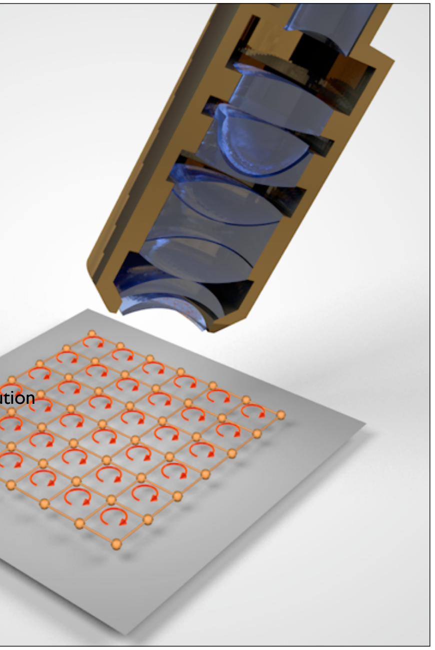

Gauge Field Team

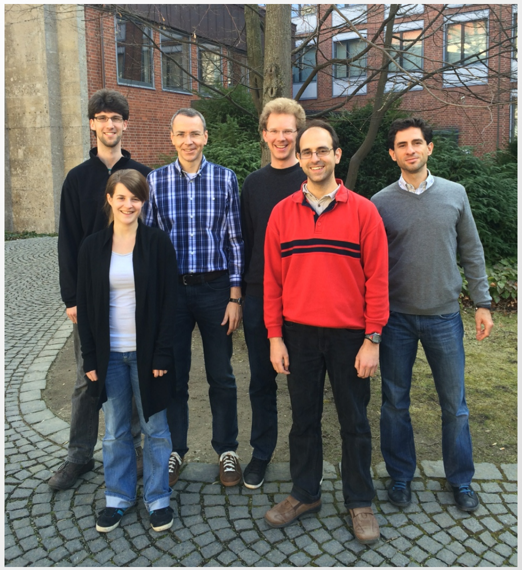

From left to right:

Christian Schweizer
Monika Aidelsburger
I.B.
Michael Lohse
Marcos Atala
Julio Barreiro

Thouless Quantum Pump

Topological Charge Pumping

- Quantized transport of charge by adiabatic periodic variation of Hamiltonian
- Transported charge related to topological invariant

$$x = \nu_n d_l$$

with $\nu_n = \frac{1}{2\pi} \oint \Omega_n(k_x, \varphi)\, \mathrm{d}\varphi\, \mathrm{d}k_x$

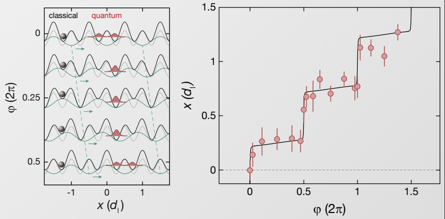

Analogy to 2D quantum Hall physics

- Charge pumping in 1D superlattice is closely related to 2D IQHE
- Direct mapping in two limiting cases

Sliding lattice - Landau levels

Wannier tunneling limit - Harper-Hofstadter model

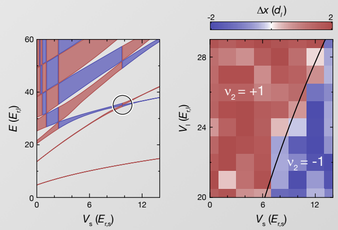

2D Berry Curvature Interferometer Team

Lucia Duca

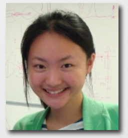

Tracy Li

Martin Reitter

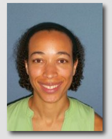

Monika Schleier-Smith

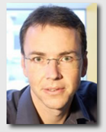

IB

Ulrich Schneider